京都大学防災研究所年報　第 49 号 C　平成 18 年 4 月
Annuals of Disas. Prev. Res. Inst., Kyoto Univ., No. 49 C, 2006

Geo-disaster Prediction and Geo-hazard Mapping in Urban and Surrounding Areas Progress Report in FY 2005

Susumu IAI, Mamoru MIMURA, Masahiro CHIGIRA, Toshitaka KAMAI, Roy, C. SIDLE, Hiroshi SUWA, Takashi SAITO, and Tetsuo TOBITA

Synopsis

Urban development rapidly expanding from lowland to surrounding hills and mountains poses increasing risks in geo-hazards, including liquefaction during earthquakes, and failure of artificial and natural slopes. Objective of this study is to develop methodologies for assessing vulnerability to these hazards, and technologies for improving the performance of geotechnical works in urban areas. This paper summarizes the results of the study with respect to (1) the use of geotechnical data base for urban areas for assessing vulnerability to liquefaction hazards and identifying priority areas for improvement, (2) prediction of large landslides for hazard mapping, and (3) landslides induced historical earthquake in ancient tomb mound.

Keywords: environment, geo-disasters, hazard mapping, urban area, hillslopes, mountains, ancient tomb mound

1. Introduction

Urban areas were highly developed in lowland and rapidly expanding toward surrounding hills and mountains. The rapid expansion causes increasing hazards associated with geological and geotechnical process. In particular, liquefaction during earthquakes causes potential risks to infrastructures in urban areas. Failure of artificial and natural slopes poses potential threats to residents and communities. Objective of this study is to develop methodologies for assessing vulnerability to these hazards, and to propose techniques for improving the performance of geotechnical works in urban areas.

This paper summarizes the results focusing on the following priority issues.

(1) Geotechnical data base for urban areas can be invaluable engineering resources for assessing vulnerability of urban areas to geotechnical hazards. An example is the data base covering the urban areas developed over Osaka Bay and Kyoto areas in Japan. This data base encompasses 38,000 on shore boring data and 4,200 boring data off shore and coastal areas. Altogether the data base can be appropriate bases for assessing liquefaction potential in Osaka and Kyoto areas. How the data base can be applied in practice of hazards assessment will be reviewed in this study.

(2) Geological and geomorphological investigations of large landslides induced by recent rainstorms in order to predict potential sites of large landslides besides shallow landslide, of which hazard could be evaluated in a wide area.

(3) Descriptions about landsliding process of the ancient large scale fill, the tomb mound, for long term stability assessment of large-scale embankments induced by strong earthquake motion in urban regions.

2. Assessment of Liquefaction Based on the Geotechnical Database

2.1 Introduction

Geotechnical database plays a significant role to investigate the regional subsoil conditions prior to detailed investigation. Geo-Database Information Committee in Kansai has developed the geotechnical database in Kansai area (Kansai Branch of JSSMFE, 1992, Geo-Database Information Committee of Kansai, 1998, 2002). For the development of the database, urban area has been focused because of its social, economical importance. 38,000 boring data was collected and digitized. Furthermore, Research Committee on Ground in Osaka Bay (2002) has developed Geotechnical database for marine foundations in Osaka Bay with 4,200 borehole data. In this report, the Geo-databases for Kansai urban area, such as Osaka, Kobe and Kyoto are introduced. Cross-sectional view of the required underground can easily be drawn on PC together with various soil properties such as classification, gradation, the thickness of each layer, ground water level, N_{SPT} values and so on. The regional geotechnical characteristics can easily be grasped by the distribution of those soil properties. As for the geotechnical disasters due to earthquake, liquefaction is one of the best known and symbolic. Then, the application of the Geo-database to assessment of liquefaction potential for urban areas is explained. The simplified procedure based on the N_{SPT} values is used to evaluate the liquefaction potential for Kobe area and the calculated results are validated by comparing with the actual records of liquefaction occurrence due to the 1995 Hyogoken-Nambu Earthquake. The method is extended to apply to predict the liquefaction potential of Kyoto Basin. Geotechnical hazard maps both for Kobe and Kyoto are shown in terms of the distribution of the critical acceleration for the occurrence of liquefaction. Based on those performances, the usefulness of the Geo-database and its applicability to geotechnical engineering and disaster mitigation engineering are discussed.

2.2 Kansai Geo-informatic Database

The Kansai Geo-informatic Database has been constructed by collecting a large amount of borehole investigation data obtained in many projects of urban construction in Kansai area. Originally there are the independent database in the inland area in Kansai with 38,000 borehole data as shown in Fig. 1 and the Geotechnical Database in the Osaka Bay area with 4,300 borehole data as shown in Fig. 2.

Those two databases were combined together and has become the Kansai Geo-informatic Database (GIbase) with 42,000 borehole data since 2003. The GIbase has utilized to assess the long-term deformation of the reclaimed marine foundations in Osaka Bay (Mimura and Jang, 2004, Yamamoto et al., 2004) as well as the liquefaction potential of sandy deposits (Oka et al., 1999, Mimura and Yamamoto, 2002). In the next section, the adopted procedure for assessing liquefaction potential of Kansai area followed by the

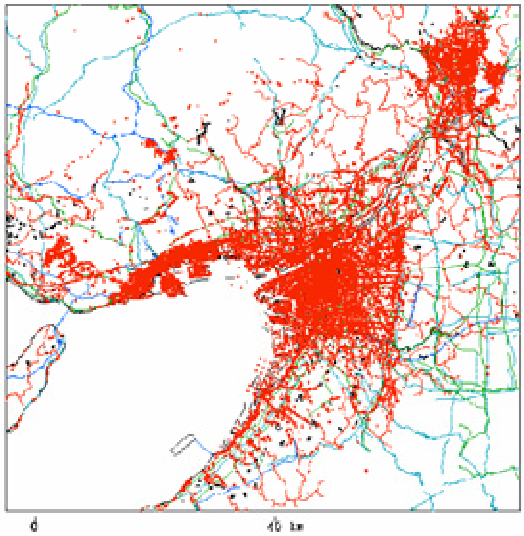

Fig. 1 Locations of boreholes in the Geotechnical Database in the inland area on Kansai

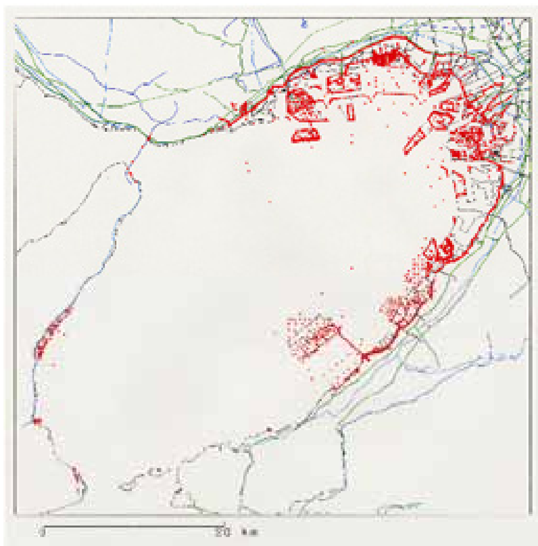

Fig. 2 Locations of boreholes in the Geotechnical Database in the Osaka Bay Area

calculated performance.

2.3 Adopted Procedure to Assess Liquefaction

Liquefaction has been highlighted since serious disaster induced by liquefaction occurred at Niigata Earthquake and Alaska Earthquake in 1964. A number of procedures for assessing liquefaction have been proposed and updated on the basis of the records of liquefaction by earthquakes taking place one after another. Laboratory tests such as undrained cyclic triaxial tests on reconstituted sand specimen have played significant roles for those studies on liquefaction. It is true that the experimental approach is important to know the mechanism of liquefaction, but the results from laboratory tests often have not provided a reasonable solution for the actual liquefaction disaster because liquefaction in the field is definitely the boundary value problem far from the laboratory conditions.

In the practical sense, the regional distribution of hazardous area against liquefaction due to earthquake can provide very important and useful information for disaster mitigation. For this purpose, geo-database can function efficiently. Here, simplified procedure assessing liquefaction potential is introduced and applied to evaluate the regional liquefaction potential based on the Geo-database. The calculated performance is validated by comparing with the actual records of liquefaction occurrence in Kobe area during 1995 Hyogoken-Nambu Earthquake. Then the predicted performance is also shown for Kyoto Basin.

The simplified procedure assessing liquefaction potential used in the present paper is a so-called F_L method specified in the "Specifications for highway bridges" by Japan Road Association (1996). This method has commonly used in Japan for designing the foundations. First, the safety factor against liquefaction, F_L is defined as follows:

$$F_L = R/L \tag{1}$$

Here, R denotes a liquefaction resistance and calculated by $R = c_w \cdot R_L$. The parameter, c_w is a correction factor depending on the type of earthquake. R_L is a cyclic stress ratio defining liquefaction in the laboratory. This parameter is usually derived from N_{SPT} values from standard penetration test (SPT) because it is not so common to carry out the undrained triaxial cyclic test on good quality sand samples. SPT is a simple and economical method to know the resistance of the foundation ground in the field, and commonly carried out for subsoil investigation. Naturally the Geo-database has the data of N_{SPT} profiles for almost all boring logs. Therefore, it is advantageous to introduce the present procedure for liquefaction assessment based on the N_{SPT} values. R_L can be calculated by the following equations:

$$\mathbf{R_L} = \begin{cases} 0.0082 \cdot \sqrt{\mathbf{N_a}/1.7} \cdots\cdots\cdots\cdots (\mathbf{N_a} < 14) \\ 0.0082 \cdot \sqrt{\mathbf{N_a}/1.7} + 1.6 \times 10^{-6} \cdot (\mathbf{N_a} - 14)^{4.5} \\ \cdots\cdots\cdots\cdots\cdots\cdots (\mathbf{N_a} \geq 14) \end{cases} \tag{2}$$

Here, N_a is a corrected N_{SPT} value in terms of the effect of fine components and expressed as follows:

$$\mathbf{N_a} = \mathbf{c}_1 \cdot \mathbf{N}_1 + \mathbf{c}_2 \qquad \text{(for sand)} \tag{3}$$

$$\mathbf{N_a} = [1 - 0.36 \log_{10}(\mathbf{D}_{50}/2)] \cdot \mathbf{N}_1 \qquad \text{(for gravel)} \tag{4}$$

Here, N_1 is a corrected N_{SPT} value in terms of confining stress. As is easily known, N_a can be calculated with mean particle size, D_{50} (in mm) and N_1 whereas more effect of fine components should be taken into account for sand with the correction coefficients c_1 and c_2. The coefficients c_1 and c_2 are assumed as follows:

$$\mathbf{c}_1 = \begin{cases} 1 \cdots\cdots\cdots (0\% \leq \mathbf{FC} \leq 10\%) \\ (\mathbf{FC} + 40)/50 \cdots (10\% \leq \mathbf{FC} \leq 60\%) \\ \mathbf{FC}/20 - 1 \cdots\cdots (60\% \leq \mathbf{FC}) \end{cases} \tag{5}$$

$$\mathbf{c}_2 = \begin{cases} 0 \cdots\cdots (0\% \leq \mathbf{FC} \leq 10\%) \\ (\mathbf{FC} - 10)/18 \cdots (10\% \leq \mathbf{FC}) \end{cases} \tag{6}$$

Here FC denotes fine components less than 74μm of diameter included in sand. As stated here, the liquefaction resistance, R_L can be derived from N_{SPT} values.

The parameter, L denotes shear stress ratio mobilized in the ground during an earthquake and is expressed in the following form:

$$\mathbf{L} = \mathbf{r_d} \cdot \mathbf{c_z} \cdot \mathbf{k_{hG}} \cdot \frac{\sigma_v}{\sigma'_v} \tag{7}$$

Here, σ_v and σ'_v are total and effective overburden stresses in kgf/cm^2, c_z is a regional correction factor (c_z = 1.0 for Osaka, Kobe and Kyoto) that is determined on the basis of the probability of earthquake occurrence, k_{hG} is a horizontal seismic coefficient at the ground surface. The parameter, r_d is a reduction factor of the shear stress ratio during an earthquake in the vertical direction to consider the non-rigid response of the ground and expressed as follows:

$$\mathbf{r_d} = 1.0 - 0.015 \cdot \mathbf{z} \qquad (8)$$

Here, z denotes a depth from the ground surface. A soil layer with F_L value larger than 1.0 is considered to be non-liquefiable while liquefaction potentially takes place in the case of $\mathbf{F_L} \leq 1.0$. It is true that F_L denotes the safety factor at a certain depth but the integrated safety factor, P_L (Fig. 3) is considered to represent the liquefaction of mass foundation, which directly induces serious geotechnical disaster. In the sense, P_L has been selected as the index for assessing liquefaction potential of regional ground in this paper. The integrated safety factor, P_L against liquefaction is defined as follows (Iwasaki et al., 1980):

$$\mathbf{P_L} = \int_0^{20} \mathbf{F_L} \cdot \mathbf{w(z)dz} \qquad (9)$$

Here, w is a weighting function in terms of depth. Values of F_L are determined to be zero for $\mathbf{F_L} \geq 1.0$ whereas 1- F_L for F_L <1.0.

2.4 Calculated performance and comparison with the measured results

The distribution of the critical acceleration (P_L=15) to induce liquefaction is shown in Fig. 4 against the scenario near field earthquake due to the failure of faults (Type-2). It is found that the central part of Kyoto is very tough against liquefaction with the required values of acceleration is 800 gal. On the contrary, 300 to 700 gal of the critical acceleration can be seen in the southern part. Particularly, low values of the critical acceleration are distributed along the rivers because a large amount of sand has been carried by those rivers and sedimented. Furthermore, floodplain has also been developed around the main flow of those rivers. Huge acceleration is certainly expected to be generated in the case of near field earthquake due to failure of faults. During the 1995 Hyogoken-Nambu Earthquake, more than 400 gal of acceleration was monitored in the natural deposits of Kobe and the adjacent cities (Japanese Geotechnical Society, 1995). In the sense, we should be prepared to undergo the acceleration of around 500 to 600 gal. From these results, serious liquefaction and its induced geotechnical disasters possibly take place in the southern

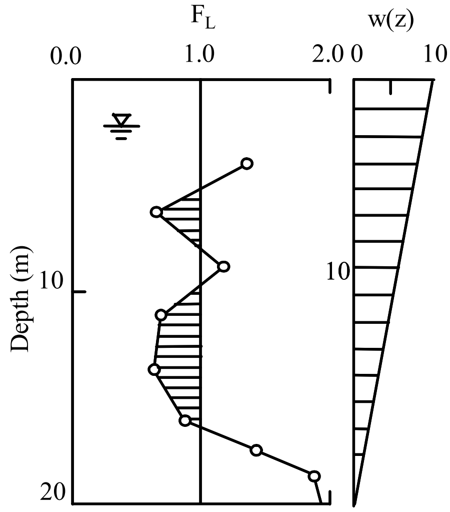

Fig. 3 Derivation of the Integrated Safety factor, P_L for Occurrence of Liquefaction

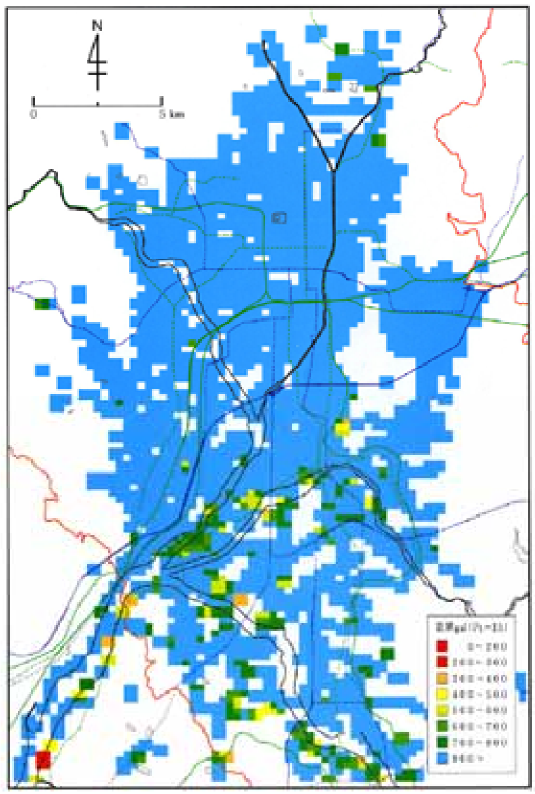

Fig. 4 Calculated Acceleration to Induce Liquefaction in terms of P_L=15 in Kyoto Basin

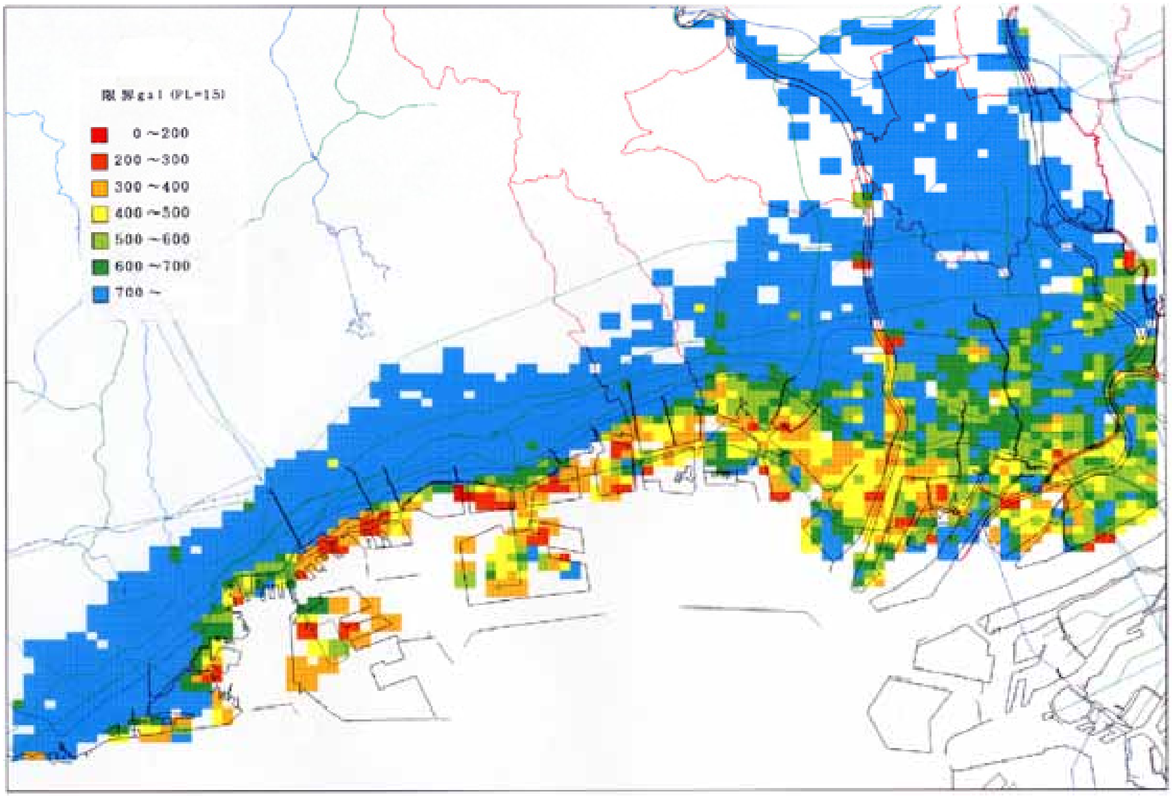

Fig. 5 Calculated Acceleration to Induce Liquefaction in terms of P_L=15 in Kobe to Hanshin Area

part of Kyoto Basin, particularly attention should be paid to the areas along the rivers.

The calculated distribution of critical acceleration to induce liquefaction in Kobe to Hanshin area is shown in Fig. 5. As is easily understood from the figure that liquefaction does not easily take place in the mountain site where more than 700 gal of acceleration is required for liquefaction occurrence. In contrast, in the lowland along the coastal line, the ground is ready for liquefy with relatively low values of acceleration. The calculated acceleration to induce liquefaction can be a hazard map against liquefaction. The actual record for occurrence of liquefaction during 1995 Hyokoken-Nambu Earthquake is found to be well described by the calculated performance shown in Fig. 5 (Mimura and Yamamoto, 2002).

2.5 Summary

Practical application in terms of assessing the regional liquefaction potential of urban area has been carried out on the basis of the Geo-database. The simplified procedure has been adopted considering that boring data normally contain only primary soil properties, such as soil classification, grading, N_{SPT} values etc. The predicted liquefaction potential in terms of P_L values were validated by comparing with the actual records of liquefaction occurrence during the 1995 Hyogo-ken Nambu Earthquake. The calculated distribution of liquefied blocks agreed well to the actual records of liquefied area in Kobe and the adjacent area. The Geo-database has played a significant role to obtain this reasonable description of liquefaction potential. Based on this validation, the liquefaction potential of Kyoto Basin was also assessed with the present scheme. In the case of Kyoto Basin, although the southern part where we have thick and weak Holocene deposits was found to possibly liquefy due to near field earthquake. In the sense of disaster mitigation, a due consideration is necessary for the possible earthquake induced geotechnical disasters and the countermeasures against them. For this purpose, the present Geo-database is versatile and should be widely utilized.

3. Prediction of catastrophic large landslide sites

3.1. Introduction

Prediction of landslide site and hazard mapping have been urging issues to mitigate landslide disaster and several approaches have been proposed for the hazard mapping: landslide maps, statistical "black-box" approaches (Carrarra, 1983), and process-based (geotechnical) models (Okimura and Ichikawa, 1985; Dhakal and Sidle, 2004). Landslide maps are made for locating potential landslide sites. Statistical "black-box" approach analyzes

the relation between landslides and other stability factors, such as geology, geomorphology, seismicity, and climate (Guzzetti et al., 1999). This method also needs a precise landslide distribution map. Process-based model is usually applied to shallow landslides, but it must assume surface structure and geotechnical properties, of which special variation could not be overcome.

Landslide maps, which are firstly necessary for the hazard mapping as stated above, may be divided into two types, one is a map showing the distribution of landslide scars of slope failures, which mean that most of the moving materials moved out of the source area and settled in another place. The other is a map showing the distribution of landslide mass, most of which still remains in its source area and have potential of future movement. The first type of landslide map does not show potential future landslide sites, because moving materials are already stabilized, but the density of landslide scars indicates the aerial hazard level of future landslide. The maps being published from the National Research Institute for Earth Science and Disaster Prevention of Japan are of the latter and are effective for the prediction of reactivating type of landslides. 1997 Sumikawa landslide and many of the landslides induced by the 2004 Mid-Niigata prefecture earthquake were reactivated landslides that were shown in their maps (Chigira et al., 1998; Chigira and Yagi, 2005). However, not all landslides have been reactivated so rating of potential landslides is necessary. In addition, many catastrophic landslides occurred on slopes without characteristic morphology of landslides, indicating the incipient stage of landslides is important for the prediction of catastrophic landslides.

We focused on specific potential sites of catastrophic large landslides (rock slides) this year as one of the major projects proceeded as one of the COE program on the basis of recent catastrophic landslides induced by rainstorms in Japan. Other types of mass movement, such as rock fall, debris flow, and creep, are not included in this paper.

Table 1 Large landslides induced by recent rainstorms.

Rainstorm	Location	Slope length (m)	Slope gradient (°)	Volume (m^3)	Geology	Causes	Precursory landform
2005 Typhoon 14	Koba	260	30	429,000	Mudstone	Shear zone	Scarplet and convex slope
	KobaNorth	250	35	1,125,000	Sandstone	High angle fault surface	Scarplet and convex slope
	Matsuoshin	304	34	863,000	Alternating beds of sandstone and mudstone	Cataclinal slope creep	Scarplet and convex slope
	Shimato	140	46	333,000	Sandstone	Shear zone	Scarplet and convex slope
	Nonoo	500	45	3,300,000	Alternating beds of sandstone and mudstone	Creep	Scarplet and convex slope
2004 Typhoon 21	Kasugadani	215	40	600,000	Chert and mudstone	Shear surface	Scarplet
	Takidani	90		8,000	Green stone	Wedge-shaped fault surfaces	None
	Kotaki	45	33	5,000	Mudstone	Cataclinal slope	None
	Ooi	80	40	50,000	Mudstone	Buckling	None
2004 Typhoon 14	Arakawa*	240	32	170,000	Pelitic schist	Cataclinal shear surface	Scarplet and convex slope

*: from Takayanagi and Fujisaki (2005)

3.2. Precursory slope deformation before large, catastrophic landslides

Large, catastrophic landslides are usually preceded by slope deformation, except for those induced by earthquakes in pyroclastics or saturated sand. However, slope deformations before landslide events have not been studied for many cases notwithstanding their importance. Recent experiences of large landslides induced by rainstorms in Japan suggest that landslides larger than 100,000 m3 in volume seem to be preceded by slope deformations, which could be detected by using aerial photographs (Table 1).

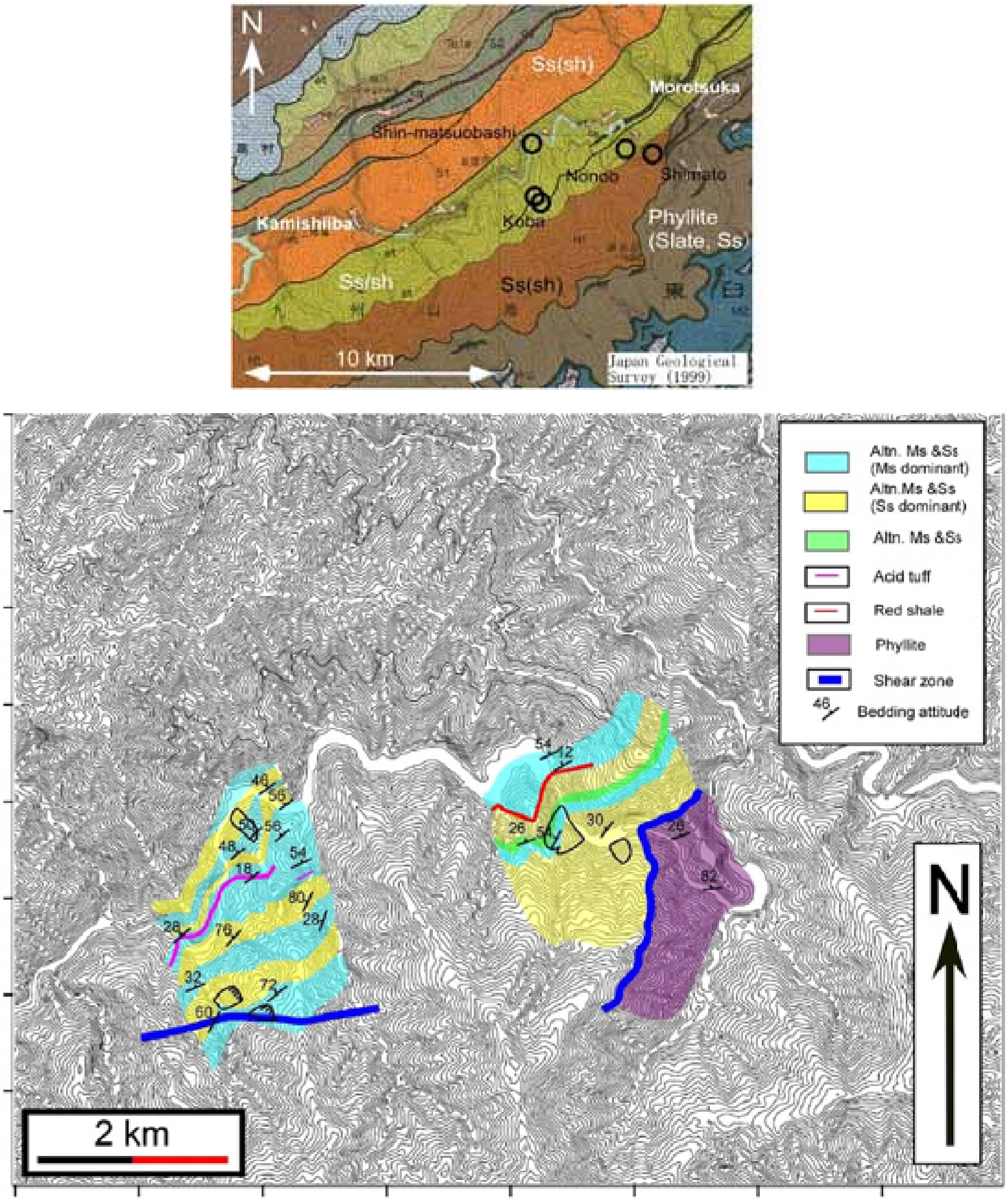

Fig. 6 Geologic map around large landslides along the Mimi River, central Kyushu. Circles with names indicate large landslide sites.

Following is the case study for large landslides induced by 2005 typhoon 14 in Kyushu Island, Japan. Typhoon 14 hit Kyushu Island on September 6 in 2005, inducing many large landslides. Particularly, along the Mimi River in central Kyushu, where precipitation reached about 1000 mm within two days, four large landslides occurred with volumes from 330 thousand cubic meters to approximately 3.3 million cubic meters (Fig. 6). Geological and geomorphological investigation elucidated that these landslides occurred under a similar geomorphological condition and that they were preceded by slope deformation that could be identified from aerial photographs. This area is underlain by the Shimanto Group of Cretaceous age, which consists mainly of sandstone and mudstone. All of these four landslides occurred on slopes just below a knick line, which lies 200-250 m above the riverbed (Fig. 7). Ridges that descend valleyward incline 10 to 30 degrees above the knick line and 40 or more degrees below it. The knick line can be traced along the Mimi River more than 10 km across geological boundaries, suggesting that it was made by long-term denudation process probably resulted from the increase of uplift rate in a geological time. In addition, all of the four landslides had scarplets on top of the slide mass before the landslide of this time. Figures 8 and 9 exemplify the geomorphic features before and after the landslide. The facts that the large landslides located just below the knick line and that scarplets or landslide scarp had been made before the slide of this time indicate that slope deformation already began in the landslides of this time because the slopes nearby the Mimi River had been under gravitationally unstable state since the erosion rate increased. Mass rock creep structures, which were observed within the landslides, also indicate the previous slope deformation.

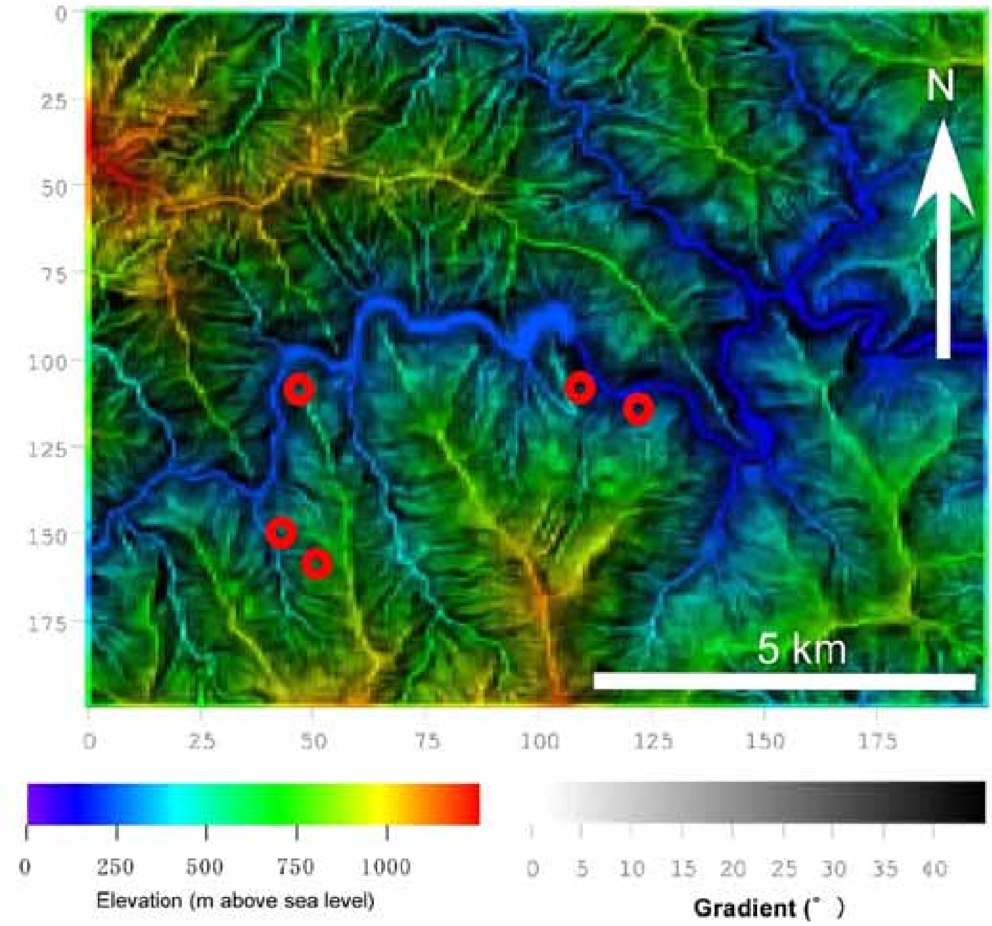

Fig. 7 Geologic map around large landslides along the Mimi River, central Kyushu. Circles with names indicate large landslide sites.

Fig. 8 Oblique views of landslides at Shin-matsuobashi (left) and Nonoo and Shimato (right). Photo by Asia Air Survey corporation.

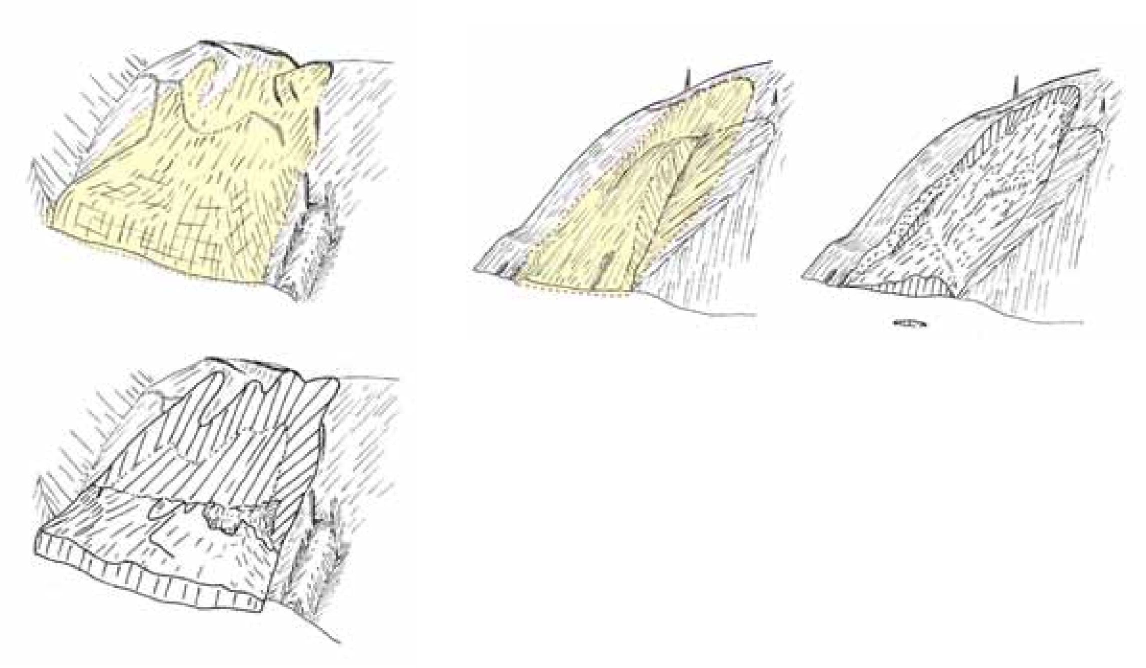

Fig. 9 Geomorphological sketches showing before and after the landslide of September 6, 2005 along Mimi River. Left :Nonoo; Right: Shin-matsuobashi. Shaded areas in the sketches before the event present the areas of landslide.

3.3. Summary

Shallow landslides could not be located precisely, but large landslide sites could be predicted from geological and geomorphological features. We analyzed geology and geomorphology of large catastrophic landslides induced by recent rainstorms in Japan and found that the landslides larger than 100,000 m3 in volume were preceded by slope deformations, which could be identified on aerial photographs.

4. Landslides on ancient burial mounds induced by the 16th century earthquake in the Kinki district, Japan

4.1 Introduction

Kofun, ancient burial tomb with double mounds, are not only famous-historical monuments of East Asia dating from 3 to 7th century AD, but also impressive large-scale fill structures that were constructed across Japan and overlap the urban regions in our modern time. Large-scale Kofun mounds were made for chiefs of powerful clans or Emperors who were at the top of the hierarchy in the ancient society. Landslides are often found on Kofun mounds. These ground failures may be used as lessons providing valuable information on both landslide mechanisms and risk mitigation of earthquake disaster due to the following reasons:

1. The original topography before landsliding can easily be recognized because the Kofun mounds have strictly confined geometries. Thus, it is easy to locate areas affected by landslides, and determine the scale of the landslides.
2. Total cross sections from the surface to beneath the slip surface of the landslides can be observed in trenches dug in conjunction with archaeological surveys.
3. The mounds were well compacted in order to remain stable during rainfall and minor earthquakes. However, large-scale earthquakes triggered landslides on the Kofun mounds, making them a data bank for investigating historical earthquakes.
4. At present, the Kofun mounds are surrounded by urban districts, and the landslides on these mounds reflect the magnitude of historical earthquake hazards

indicating therefore the risk of future disasters of landfills, embankments and other major soil constructions in these urban areas.

5. The available evaluation time frame for the stability of embankments is commonly restricted to a few decades, however, landslides on Kofun mounds provide a unique opportunity to investigate the long-term stability of earth structures.

The opportunity to investigate landslides on Kofun mounds is highly restricted because they are usually important cultural heritages nominated by the Government, however, in collaboration with archaeologists we were allowed to conduct detailed investigations on the Imashiro-zuka in the northern Osaka urban district. The mounds is located along active fault systems at the border of the northern Osaka sedimentary basin, and likely collapsed due to the historical earthquake in the 16th century. Obvious interior structures of the landslides and deformations of the mound were revealed in the trenches constructed during archaeological surveys from 2000 to 2004. This was a unique opportunity to observe the entire cross section of a landslide with a clearly known triggering mechanism. Our investigations provide not only the first detailed description of landslides on the mounds, but also valuable case studies of the collapse of modern large-scale embankments induced by strong earthquake motion in urban regions. Recent urban developments, mainly housing, roads and lifeline constructions, thoroughly invaded the surroundings of the mound. The landslides on the mound stand as illustrative examples of the risk associated with unstable ground conditions in the urban region of the Kinki district.

4.2 Active fault systems and distribution of Kofun mounds

Tomb mounds including the Imashiro-zuka are distributed around the northern marginal region of the sedimentary basin of the Osaka Group; the Pliocene-Pleistocene strata in Kinki district. The margin consists of a series of faults belonging to two major active fault systems, the Arima-Takatsuki tectonic line and the Rokkou fault system. Both mounds are situated along this series of active faults with the Imashiro-zuka along the Arima-Takatsuki tectonic line and the Nishimotome-zuka in Kobe along the Rokkou active fault system (Fig. 10).

The Arima-Takatsuki tectonic line is composed of active faults that are arranged in rows and branches, and covers 55 km at the surface from Arima hot spring to Takatsuki city. In the eastern part, from Takarazuka to Takatsuki, two parallel faults form a graben called the Minou low land. The movement of these faults involves a right lateral slip with a northern side rise, and they are evaluated as having one of highest degrees of fault movement activity in Japan. The eastern part, from Takarazuka to Takatsuki, moved at least three times within the recent three thousand years, leading to an activity interval of one thousand years. The latest activity of this tectonic line caused the Keicho-Fushimi earthquake in 1596.

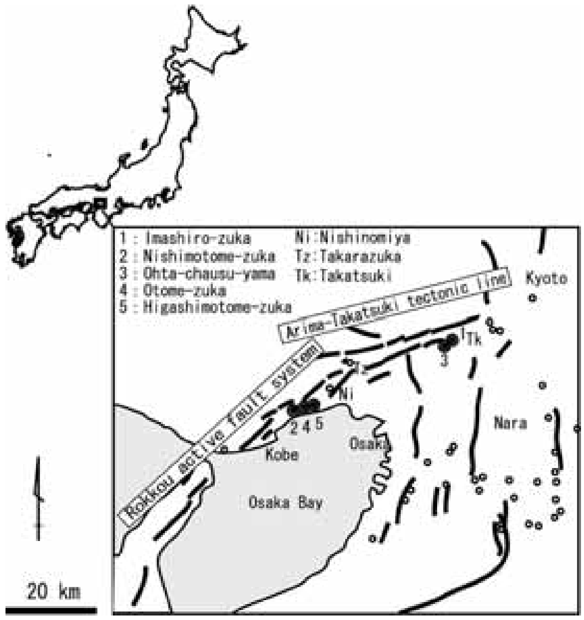

Fig.10 Distribution of ancient mounds and active fault system of the Kinki district

The Rokkou active fault system is connected to the Arima- Takatsuki tectonic line at the east side of the Rokkou Mountains in Minou city. This fault system is composed of active faults related to the rising of the Rokkou Mountains, and continues 71 km southeast to Awaji Island. The movement of these faults includes a right lateral slip with a north –western side rise. The 1995 Hyougoken-nanbu earthquake (i.e., Kobe earthquake) occurred along a 40 km stretch of this part of the fault system, from Nishinomiya city to the northern part of Awaji Island, however, the latest movement of the entire fault system is estimated to have occurred in the 16th century.

Both the Arima-Takatsuki tectonic line and the Rokkou active fault system, are often subjected to linked movements, and have induced some historically huge-scaled (M7.5 –M8) inland earthquakes larger than the 1995 Hyougoken-nanbu earthquake. The latest huge-scale earthquake is considered to be the Keichou-Fushimi earthquake in 1596.

4.3 The Imashiro-zuka

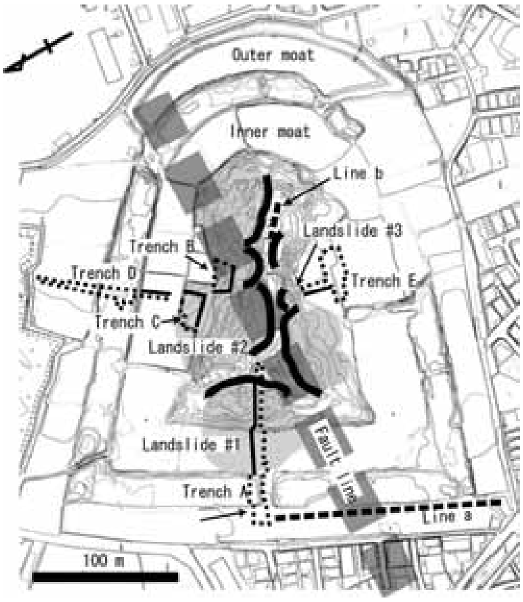

Fig.11 Landslides on the mound and earthquake fault in 1596

The Imashiro-zuka located in Takatsuki City is one of the largest tomb mounds of the 6th century in the northern Osaka region. Based on archaeological research, it is considered to be the tomb of the Great Emperor Keitai who died in 531 AD. The capital of the Yamato dynasty (Government of the ancient Japan) was located close to the Imashiro-zuka during the first half of the 6th century. The Imperial Household Agency of the Government has identified and listed Emperors' tombs among the many tomb mounds located in the ancient capitals of Japan. The government intends to preserve all Emperor's tombs from excavations, and thus does not permit investigations on these. The Imashiro-zuka failed to be listed by the Imperial Household Agency as an Emperor's tomb because of its deformed shape. Instead of the Imashiro-zuka, a mound of better shape, Ohta-chausu-yama, was officially appointed Emperor Keitai's tomb. Archaeological research on Imashiro-zuka started in 1996. This is the first detailed research on an Emperor's tomb mound, and culminated in remarkable archaeological achievements, including numerous ceramics. It was also discovered that a landslide drastically deformed the tomb mound.

The Imashiro-zuka mound was built on alluvial sediments consisting of clay and fan deposits that fill the Minou lowland graben structure bordered by the Arima-Takatsuki tectonic line. The Ai fault which constitutes the southern flank of the graben structure, is

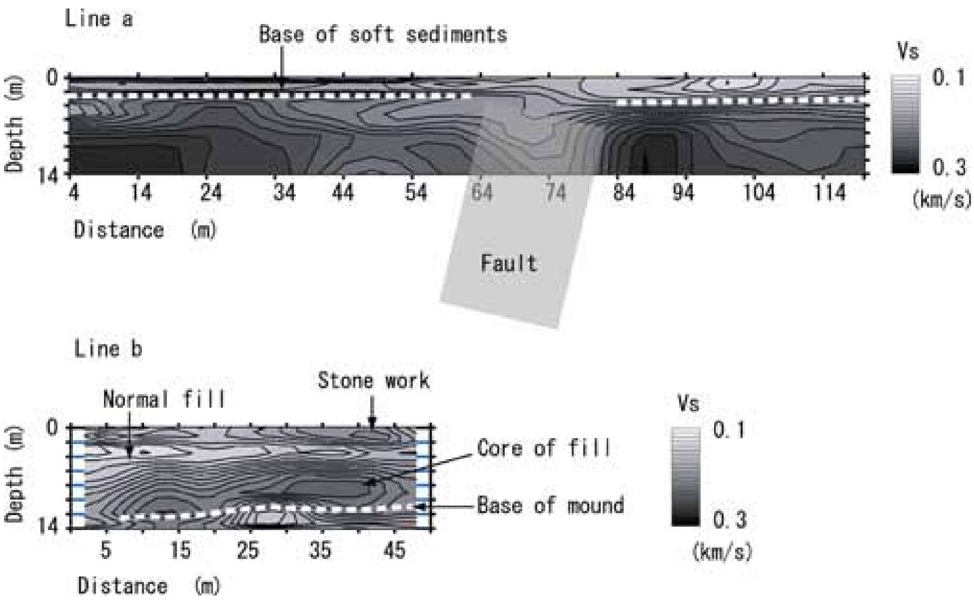

Fig.12 Vs cross-section of the mound

invisible on the surface up to 1 km west of the Imashiro-zuka, however, the mound is located directly on the strike of the fault(Fig.11). Fig.12 (line a) shows an S-wave velocity (Vs) cross section along the northwest corner of the outer moat based on the results of high precision surface-wave explorations (Hayashi and Suzuki, 2001). A distinct gap in the surface layers is identified in this section, indicating major post depositional vertical movement, as shown in Fig.12 (line a). In the northern end of the profile (left hand side) the surface consists of 3-4 m thick soft alluvial strata (Vs =130-160 m/s), however, the surface of the southern part consists of hard (over 200 m/s) strata. The north side of the Ai fault moved relatively downward, and the gap between the top surface layers are the results of recent fault activities, indicating that the Ai fault of the Arima-Takatsuki tectonic line runs right below the mound. Trench investigations 2 km west of the Imashiro-zuka conducted by the Geological Survey of Japan revealed that the Ai fault during the 1596 Keicho-Fushimi earthquake moved at least 3 meters in right lateral direction and several centimeters in south bound vertical direction. This means that the Imashiro-zuka is one of the largest fill structures located in the region of the highest seismic activity in the world.

4.4 Structure of the mound

The plan view of the Imashiro-zuka mound is keyhole shaped resulting from a combination of a front square mound and a rear circle mound (Fig. 11). This keyhole shape is the most popular and original shape of the ancient tomb mounds in Japan. The tomb, 186 m long, 100 to 141 m wide and 10 to 15 m high, is surrounded by a 1 to 4 m deep water-filled double moat. The mound sustained an artificial landform change by the Lord Nobunaga in the 16th century who constructed a fortress for his troops on the mound.

The mound is composed of two kinds of fills: a core part fill and a normal fill. The core fill is easily distinguished from the normal fill because of clear color differences, stiffness, and density. The core part fill, produced from mixtures of fine sand, silty clay and charcoal, is grey colored, and very dense as a result of intensive compaction; it was difficult to excavate even by a small excavator. The wet density of soil blocks ranges from 2.02 to 2.06 g/cm3, and the void ratio ranges from 0.514 to 0.561. The normal fill is brown, and has only been moderately compacted. Fig.12 (line b) shows an S-wave velocity cross section from the top of the back circle to the necking part of the mound. The foundation bed of alluvial strata with *V*s ranging from 150 to 200 m/s is covered with core part fill which has a *V*s over 200 m/s. The core part of the mound is covered with the normal fill with *V*s of 110 to 150 m/s. The higher anomaly at the top-right hand side near the surface is caused by refraction of the stonework of the chamber. The thickness of the covering normal fill decreases towards the marginal part of the mound.

4.5 Overview of Landslides

Landslide body

The head scarps of the landslides are easily distinguished on the mound. Seven landslides developed on the slope of the tomb mound, however, because archaeologists did not recognize landslides on the mound until 2001 we were only able to investigate landslide #1, #2 and #3 along with the trenches distribution.

Horizontally layered small, hand-made soil blocks, approximately 40 cm wide, 40 cm long and 10 cm thick, comprised the fill (embankment) of the mound. The remains of ‘scaly mosaic’ (fish skin) structures corresponding to each soil block are oriented almost horizontally in the original non-disturbed part of the mound. Thus, deformation of these horizontal units of the scaly mosaic structure is a valid indicator of the deformation caused by landslides and other artificial disturbances of the mound.

Both landslide #1 and #2 are deep-seated landslides involving the core of the mound while landslide #3 is a shallow slope failure of the normal fill. Deformation by the deep-seated landslides reached the ridge of the mound behind the main scarps. Both types of landslides involved mass transfer in a highly fluid state after collapse, resulting in long travel length relative to the height of the mound. The deep-seated landslides are distributed mainly on the northern side of the mound which coincides with the downward side of the Ai fault indicating that the landslides were affected by differences in the geological conditions of the foundation.

Shear zones

The failure surface of the landslides developed

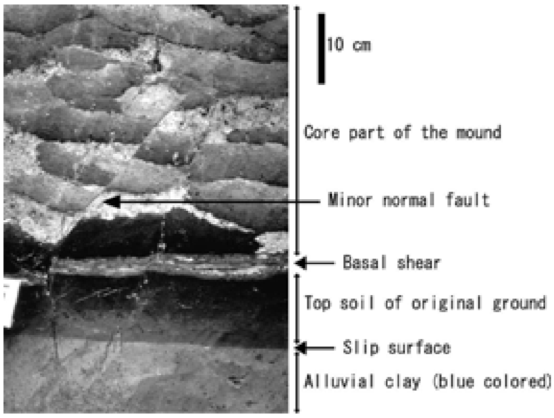

Fig.13 Shears of the landslide

mainly along the boundary between the original ground surface and the bottom of the fill of the tomb mound. There are two shear horizons in the deep-seated landslides #1 and #2 as shown in Fig. 13. The upper horizon denoted as "the basal shear", has a 1 to 4 cm thick shear zone in which the core material (fill) of the mound was crushed and thinly elongated. Relative displacement by the earthquake shaking between separated bodies having different inertia such as between the heavy mound and the alluvial foundation bed is considered to be the major cause of basal shear.

The lower shear horizon is a landslide slip surface with a smooth shear surface cutting the soft blue-colored alluvial clay and the soft bottom sediments of the moat. Because the slip surface is located below the basal shear zone and developed after the formation of latter it often intersects the basal shear horizon. The elongated structure of the soil noted in within the basal shear horizon suggests that the ground water table during landslide movement was above the basal shear horizon.

4.6 Structure of landslides #1

The main body

The depth of the slip surface is between 2 and 6 m below the surface. The base of the mound is inclined 1 to 3 degrees towards the central part of the mound in trench A, which is in the opposite direction of the normal landslide movement. It appears that this inc lination of the base is caused by ground subsidence in the alluvial clayey deposits due to excess load of the mound (Fig.14a,b,c).

The original scaly mosaic structure is maintained almost undisturbed in the main part of the landslide mass that was subjected to a limited vertical displacement of 1 to 2 m, because of the non-rotational movement of the main body of the landslide. Coherent landslide movement along the almost-horizontal slip surface can be recognized by a slight deformation of this part. In the head (upper part) of the landslide, the scaly mosaic structure of the filling material is steeply inclined (50-70 degrees) towards the central part of the mound. It is assumed that the upper part of the head of the coherent landslide body fell with a rotational movement (toppling to backward) into the open space (graben) that was formed by the landslide movement. The opposite inclination of the slip surface enhanced the movement (toppling). Based on the openings in the graben, the horizontal movement of the main part is estimated to 3-5 m.

Movement of the main part was predominately along the lower slip surface formed between the black-colored topsoil just below the mound and blue-colored alluvial clay of the foundation bed. The upper slip surface between the mound and the topsoil developed about 10 cm above the lower slip surface; however, it was displaced by several minor gravitational faults connected to the lower slip surface.

The foot

The lower half of the main body crossing the border of the moat collapsed as a rotational slump, and fell into the moat. Associated minor gravitational faults were formed behind the head scarp of the slump. Because the moat was filled with water, the landslide body got swelled as it absorbed water and spread across the inner water-filled moat as an underwater turbidity flow (Fig.14c).

A ditch, 5 m wide and 1.2 m deep, was constructed at the bottom of the moat on the mound side from the 13th to 16th century, and had been filled with ditch mud. When the landslide body of the slump moved into the ditch it caused mud to be splashed up, and the landslide body rolled up vigorously in the water. The landslide flow reached the opposite side of the moat, and the tip of the flow bent slightly upward along the flank before it terminated.

4.7 Summary

Landslides on the ancient burial mounds, Imashiro-zuka were induced by a historical earthquake initiated by tectonic movement of the active fault systems located between

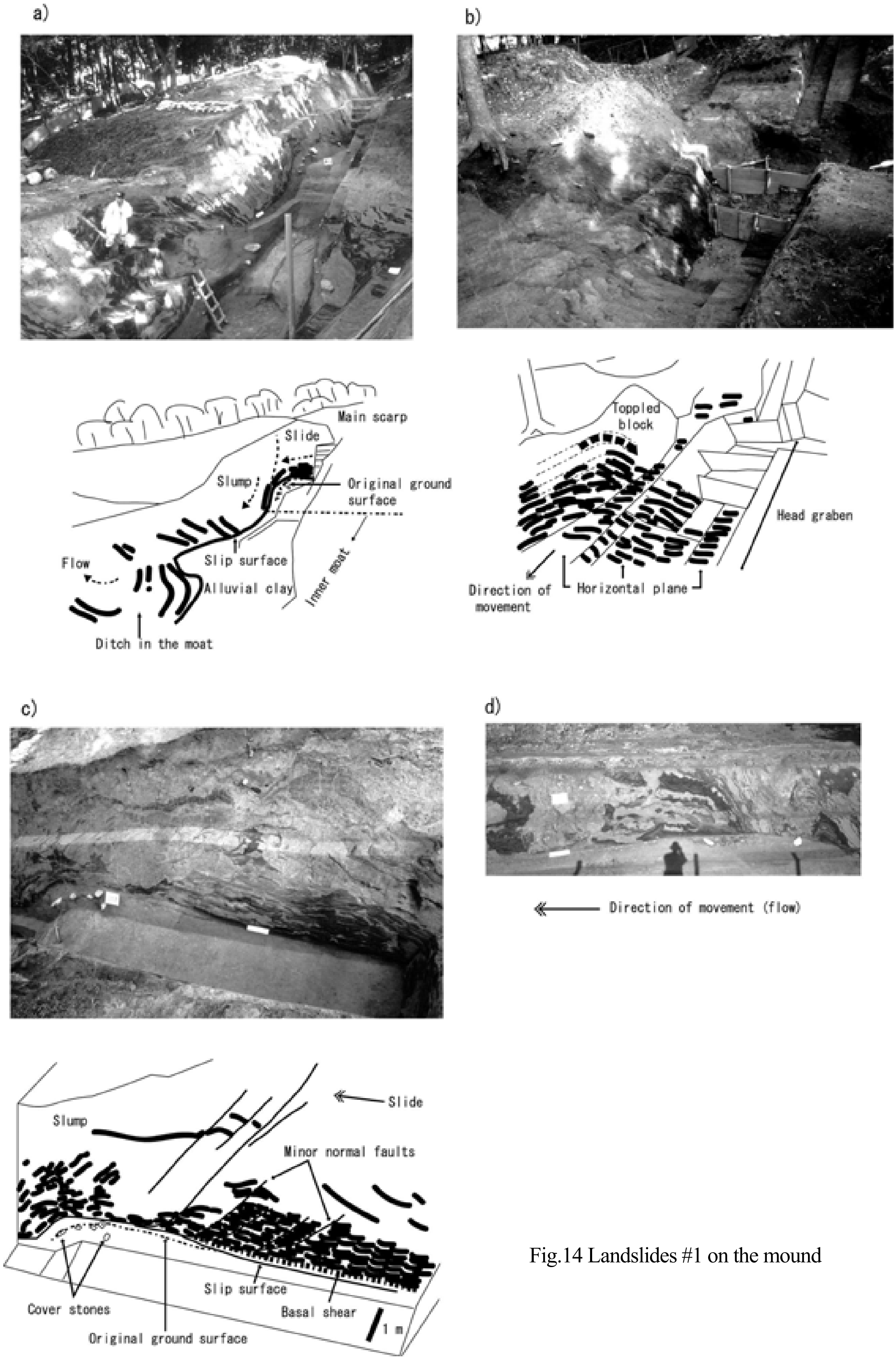

Fig.14 Landslides #1 on the mound

northern Osaka and Kobe. Obvious interior structures of landslides revealed the deformation processes of the landslide bodies, and provided significant information for discussing landslide mechanisms.

Because the ancient tomb mounds were high quality embankments (fills) even compared to modern soil structures, the mounds are still in place after 1500 years. Therefore, landslides on the mounds indicate records of the destructive earthquakes affecting the mounds and its surroundings. The ancient burial mounds in Kinki district were distributed from coastal regions to hills overlapping modern urban regions. Many of the recent artificial valley fills in urban region constructed on the soft natural deposits in the previous valleys collapsed by almost the same landslide mechanism as the Imashiro-zuka . Thus, the landslides on these ancient mounds provide important information on issues of our modern society.

5. Conclusions

Methodologies for assessing vulnerability to the geo-hazards, and techniques for improving the performance of geotechnical works in urban areas are investigated. Major results obtained from this study may be summarized as follows.

(1) The geotechnical data base, such as those developed for the urban areas in Osaka Basin and Kyoto areas, can be a powerful tool for assessing vulnerability to geo-hazards. Application of this data base to Kobe and Osaka areas with respect to liquefaction potential resulted in consistent hazard level as observed during Hyogoken-Nambu earthquake of 1995. Application of this data base to Kyoto area indicated that the southern areas of Kyoto where thick and soft Holocence deposits lay are susceptible to liquefaction when a near field earthquake occurs, and appropriate mitigation measures should be considered for this area.

(2) Geological and geomorphological investigation of large landslides induced by recent rainstorms showed that large ones exceeding about 100,000 m3 may be preceded by gravitational deformation forming scarplets, which could be used as a criteria for the prediction.

(3) Landslides on ancient burial mound, Imashiro-zuka , induced by historical earthquake related to the tectonic movement of an active fault systems located between northern Osaka and Kobe have obvious interior structures of landslides showing the deformation process of the landslides, and provide significant information for discussing landslide mechanisms. The geological conditions of the foundation of the mounds, the lithology, stiffness, and the position of the mound relative to the fault systems, contribute to the collapse of the mounds. Landslides of embankments (fills) are unavoidable over long periods of time if any weaknesses are present at the foundation of the construction, in other words, the total quality of an artificial soil structure very much depends on the conditions of its foundation bed.

Acknowledgments

This paper summarizes the results of the COE research performed by Geo-disaster Division, DPRI. Primary part of this paper, i.e. Chapters 2 through 4, is based on the contributions by the 2nd through 5th authors. The first author compiled the paper as project leader in 2005. The authors wish to express their sincere gratitude to these professors.

This research was supported by the Japanese Ministry of Education, Culture, Sports, Science and Technology (MEXT) 21st Century COE Program for DPRI, Kyoto University (No.14219301, Program Leader: Prof. Yoshiaki Kawata) as well as the Grant-in-Aid for Scientific Research (B) (2) (No. 15310129 Principal Investigator: T. Kamai, Kyoto University), Grant-in-Aid for Scientific Research (Seeds) (No. 17651098 Principal Investigator: T. Kamai, Kyoto University). Geo-database used in the present research has been developed by the Kansai Geo-informatics Network. Dr. K. Yamamoto, Geo-Research Institute co-operated to utilize the geo-database and a series of analyses for developing the hazard map.

References

Carrarra, A. (1983) A multivariate model for landslide hazard evaluation. Mathematical Geology 15, 403-426.

Chigira, M., Chiba, T. and Matsuura, S. (1998) Landslide-triggered steam explosion and debris flow in May, 1997, at the Sumikawa Spa, Akita, northern Japan. 1. General view and geological background. Landslide News, 11, 6-8.

Chigira, M. and Yagi, H. (2005) Geological and geomorphological characteristics of landslides triggered by the 2004 Niigata-ken Chuetsu Earthquake in Japan. Engineering Geology, 82, 202-221.

Dhakal, A.S. and Sidle, R.C. (2004) Distributed simulations of landslides for different rainfall conditions. Hydrological Processes, 18, 757-776.

Geo-database Information Committee of Kansai (1998): Shin Kansai Jiban (Ground of Kansai Area Especially Kobe to Hanshin), 270p., (in Japanese).

Geo-database Information Committee of Kansai (2002): Shin Kansai Jiban (Ground of Kansai Area Especially Kyoto Basin), 196p., (in Japanese).

Guzzetti, F., Carrara, A., Reichenbach, P. and Cardinali, M. (1999) Landslide hazard evaluation: a review of current techniques and their application in a multi-scale study, Central Italy. Geomorphology, 31, 181-216.

Iwasaki, T., Tatsuoka, F., Tokita, K. and Yasuda, S. (1980): Estimation of Degree of Soil Liquefaction During Earthquake, TSUCHI-TO-KISO, Vol. 28, No. 4, pp.23-29, (in Japanese).

Japanese Geotechnical Society (1995): Report on the Geotechnical Disasters During the 1995 Great Hanshin-Awaji Earthquake (in Japanese), 594p.

Mimura, M. and Jang, W.Y. (2004): Description of Time-dependent Behavior of Quasi-overconsolidated Osaka Pleistocene Clays Using Elasto-viscoplastic Finite Element Analyses, *Soils and Foundations*, Vol. 44, No. 4, pp. 41-52.

Mimura, M. and Yamamoto, K. (2002): Development of Liquefaction Potential, Proc. 2nd IKRAM Int. Geotechnical Conf., 235-252.

Oka, F., Mimura, M. and Yamamoto, K. (1999): Liquefaction due to Hyogoken-Nambu Earthquake and Prediction Methods, Proc. Symp. on the Mechanism of Liquefaction and Its procedure for prediction and Design, pp.511-516 (in Japanese).

Okimura, T. and Ichikawa, R. (1985) A prediction method for surface failures by movements of infiltrated water in a surface soil layer. Journal of Natural Disaster Science, 7, 41-51.

Research Committee on Ground in Osaka Bay (2002): Ground and Construction of Bay Area, Association of Research on Geotechnical Information in Osaka Bay, 660p. (in Japanese).

Takayanagi, T. and Fujisaki, T. (2005) Landslide by Typhoon 0421 at Arakawa in Saijo. Abstract of Geohazards and Geoenvironment, 5, 71-78. (in Japanese)

Yamamoto, K., Nagaya, J., Mimura, M. and Takeda, K. (2004): Long-term Settlement Prediction of Pleistocene Clays in Osaka Bay Based on Geotechnical Database, Proc. Int. Symp. on Engineering Practice and Performance of Soft Ground, IS-Osaka 2004, pp. 415-420.

都市および周辺地域における地盤災害予測とハザードマッピングに関する研究
平成17年度報告

井合　進・三村　衛・千木良雅弘・釜井俊孝・Sidle, R.C.
諏訪　浩・斉藤隆志・飛田哲男

要旨

低平地を中心として急速に周辺丘陵地へと拡大する都市域では，地震時液状化，宅地造成地盤崩壊，人工・自然斜面崩壊など，地盤災害の危険性が増している。本研究は，これらの地盤災害に対する都市域の脆弱性診断技術と危険度評価技術の高度化，地盤基礎構造物の性能向上技術の開発を目的とする。平成１７年度のとりまとめとして，本論文では，都市域の地盤情報データベースの地盤ハザード評価への適用，地質・地形的前兆現象による大規模崩壊の発生場所予測の可能性，都市周辺の巨大古墳に記録された地震による地すべり災害についてとりまとめた。

キーワード: 環境，危険度評価，都市域，丘陵地，山地，地盤災害，古墳